SIMULTANEOUS EFFECTS OF WATER SPRAY AND CROSSWIND ON PERFORMANCE OF NATURAL DRAFT DRY COOLING TOWER

by

Hossein AHMADIKIA [a], Mohsen SOLEIMANI [b], and Ehsan GHOLAMI [b]

[a] Department of Mechanical Engineering, University of Isfahan, Isfahan, Iran
[b] Department of Mechanical Engineering, Bu-Ali Sina University, Hamedan, Iran

Original scientific paper
DOI: 10.2298/TSCI110510134A

To investigate the effect of water spray and crosswind on the effectiveness of the natural draft dry cooling tower, a 3-D model has been developed. Efficiency of natural draft dry cooling tower is improved by water spray system at the cooling tower entrance for high ambient temperature condition with and without crosswind. The natural and forced heat convection flow inside and around the natural draft dry cooling tower is simulated numerically by solving the full Navier-Stokes equations in both air and water droplet phases. Comparison of the numerical results with 1-D analytical model and the experimental data illustrates a well-predicted heat transfer rate in the cooling tower. Applying water spray system on the cooling tower radiators enhances the cooling tower efficiency at both no wind and windy conditions. For all values of water spraying rate, natural draft dry cooling tower operate most effectively at the crosswind velocity of 3 m/s and as the wind speed continues to rise to more than 3 m/s up to 12 m/s, the tower efficiency will decrease by approximately 18%, based on no-wind condition. The heat transfer rate of radiator at wind velocity 10 m/s is 11.5% lower than that of the no wind condition. This value is 7.5% for water spray rate of 50 kg/s.

Key words: *natural draft dry cooling tower, water spray, wind, power plant*

Introduction

Cooling tower capability has a very important role to play in the efficient operation of a power plant. The ability of the designers to predict the cooling tower performance along with designing an exact condition is highly recognized. The natural draft dry cooling tower (NDDCT) offers a number of inherent advantages, such as low water consumption and reduced risk in water sources pollution specially in arid and semi-arid areas. The disadvantages of the NDDCT are in their performance high dependency on the environmental conditions especially on warm and windy days. At higher temperatures of 37 °C, the NDDCT does not operate well unless the peak coolers are turned on.

Several researchers have conducted studies on dry cooling towers of power plant both experimentally and numerically [1, 2]. As the pioneers in this field, Demuren and Rodi [3] assumed the dry cooling tower as a cylinder, modelled based on the buoyancy effects as an inlet warm airflow. Due to the improper modelling of the buoyant airflow, they could not predict the velocity and temperature profiles correctly. They did not use the Boussinesq approximation in their simulation. Bergstrom *et al.* [4] presented a 2-D code for simulating the interior of the cooling tower. Kappas [5] investigated the flow patterns and the characteristics of the dry cooling

* Corresponding author; e-mail: ahmadikia@eng.ui.ac.ir

tower with different delta angles using a 2-D model. This model assumed constant pressure drop. In his later work, Kappas [6] used a 3-D heat exchanger model, and simulated a Heller-type NDDCT. He imposed mass flow rate on the heat exchangers, with the knowledge that the natural cooling tower flow rate depends on the environmental conditions and the cooling tower characteristics. Du Preez and Kroger [2] investigated a NDDCT model by applying the crosswind effects, experimentally. They found that when the heat transfer rate is increased, the cooling towers become less sensitive to the wind effect. Du Preez and Kroger [1] simulated a NDDCT by the PHOENICS software under crosswind conditions. They found that applying wind-break walls reduced the wind effects. Al-Waked and Behnia [7] investigated the buoyant airflow through dry cooling towers by FLUENT commercial package as a solver and included the effects of wind. They reported that the wind-breakers contribute to the negative effect reduction of the wind on the tower performance. Some other researchers have presented the similar results [8-13].

The NDDCT efficiency is decreased when the ambient temperature is more than 37 °C. As the temperature increases, the energy efficiency and output power of steam power plants decrease [14]. In order to increase the cooling tower efficiency in the hottest summer days, was applied water spray at the entrance of the cooling tower to be used for peak shaving.

In this study, a more detailed model is developed for NDDCT with empirical correlations for heat transfer and pressure drop in the radiators which is able to resolve the problems regarding heat and mass transfer and air flow in all regions of the NDDCT subjected to simultaneous water spray and crosswind. For windy and high ambient temperature conditions, simultaneous effects of water spray and crosswind are studied on the NDDCT performance. The overall model predictions are compared with experimental data and the analytical results.

The geometry of a typical Heller-type NDDCT is illustrated in fig. 1. The cooling tower dimensions are 150 m × 118 m × 60 m (height × base diameter × top diameter), while height of radiators which are located around the base of the cooling tower is about 20 m. Sketch of the cooling tower including the radiators (deltas) and water spray system is shown in fig. 1. In each delta, water is sprayed in four different elevations.

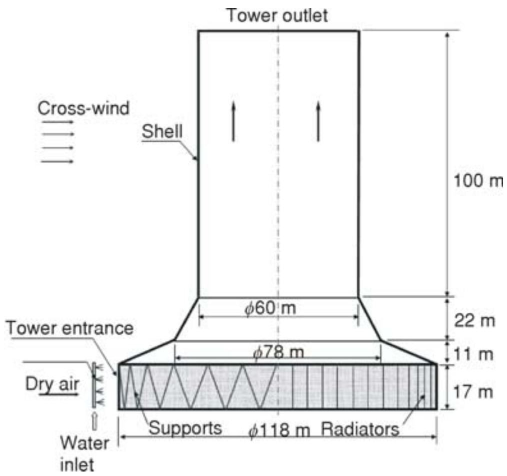

Figure 1. Sketch of the Heller-type NDDCT including radiators and spray nozzles

The governing equations

The governing equations are 3-D and incompressible steady-state flow that includes continuity, momentum, and energy along with two transport equations for turbulence modelling. An alternative approach to estimate the drift deposition is to predict both the flow field and the droplet drift patterns close to the cooling tower entrance. The air and water spray flows in the cooling tower are modelled by applying a two-phase simulation: the gas continuous phase and the discrete water droplets. The air flow is solved as a continuous phase using the Eulerian approach whereas droplet trajectories are solved as a dispersed phase using the Lagrangian approach. The continuity equation for mass conservation in Cartesian co-ordinates for steady-state flow can be given as:

$$\rho\vec{\nabla}\vec{V} = S_m \tag{1}$$

where, mass source term, due to the evaporation of droplets, S_m, is given by:

$$S_m = \frac{\Delta m_P}{m_{P,0}}\dot{m}_{p,0}\frac{1}{d\forall} \tag{2}$$

where Δm_p is the particle mass change in each volume differential $d\forall$ in a time step, $\dot{m}_{P,0}$ – the initial mass flow rate of the injected tracked particle and $m_{p,0}$ – the initial mass of the particle. For more details, refer to Kaiser *et al.* [10].

The equation for conservation of momentum can be written as:

$$\rho_a(\vec{V}\vec{\nabla})\vec{V} = -\vec{\nabla}p + \vec{\nabla}(\boldsymbol{\tau}_{eff}) - \rho_a\vec{g}\beta(T - T_{amb}) + \vec{F}_D + \vec{F}_P \tag{3}$$

where $\boldsymbol{\tau}_{eff}$ is the stress tensor which can be calculated using the following equation:

$$\boldsymbol{\tau}_{eff} = (\mu + \mu_t)S_{ij}, \quad S_{ij} = \frac{1}{2}\left(\frac{\partial V_i}{\partial x_j} + \frac{\partial V_j}{\partial x_i}\right) \tag{4}$$

The source term due to the pressure drop in the louvers and radiators, $\vec{F}_p$, is explained in next section. $\vec{F}_D$ is the source term of resistance against the air flow due to the sprayed water droplets [15-17]:

$$\vec{F}_D = \frac{18\mu_a}{\rho_P d_P^2}\frac{C_D \operatorname{Re}}{24}$$
$$\operatorname{Re} = \frac{\rho_P d_P(V_P - V_a)}{\mu_a}, \quad C_D = a_1\frac{a_2}{\operatorname{Re}} + \frac{a_3}{\sqrt{\operatorname{Re}^3}} \tag{5}$$

Morsi and Alexander [15] give the drag coefficient of spherical particle, C_D.

The equation for conservation of momentum in Cartesian co-ordinates can be written as:

$$\rho_a(\vec{V}\vec{\nabla})T = \vec{\nabla}\left[\left(\frac{\mu}{\Pr} + \frac{\mu_t}{\Pr_t}\right)\vec{\nabla}T\right] + q_r + q_v \tag{6}$$

where q_r is the heat transfer source term in the radiators deduced by e-NTU method [18-20]. Heat and mass transfer rate of a solid sphere like small water droplets is calculated by Merkel's model by balancing convective heat transfer and the droplets' evaporation rate, q_v. For more details, refer to refs. [17, 21].

Water droplets are assumed perfectly spherical. The source terms are the air resistance, gravity and the buoyancy forces. By balancing these forces, acceleration, velocity and displacement of droplets are obtained. The motion equations of the water droplets can be presented by:

$$\frac{d\vec{V}_P}{dt} = F_D(\vec{V}_a - \vec{V}_P) + \vec{g}\left(1 - \frac{\rho_a}{\rho_P}\right) + \vec{F}_t, \quad \vec{V}_P = \frac{dx}{dt} \tag{7}$$

$$\vec{F}_t = \frac{\rho_a}{\rho_P}\vec{V}_P\frac{\partial\vec{V}}{\partial r_P}, \quad \frac{d\vec{r}_P}{dt} = \vec{V}_P \tag{8}$$

where $\vec{F}_t$ is the thermophoretic force due to the heat gradient and r_p – the droplet trajectory [15-17]. The droplet trajectory is determined by advancing the droplet location over small discrete time intervals with the step-wise integration in each co-ordinate direction of eq. (7).

Here, the standard k-ε turbulence model is used for the simulations of turbulent flow. The transport equations for the turbulence kinetic energy, k and the dissipation rate, ε, are given by:

$$\rho_{\mathrm{a}}(\vec{\nabla}\vec{\nabla})k = \vec{\nabla}\left[\left(\mu + \frac{\mu_{\mathrm{t}}}{\sigma_{\mathrm{k}}}\right)\vec{\nabla}k\right] + P_{\mathrm{k}} + G_{\mathrm{b}} - \rho_{\mathrm{a}}\varepsilon \tag{9}$$

$$\rho_{\mathrm{a}}(\vec{\nabla}\vec{\nabla})\varepsilon = \vec{\nabla}\left[\left(\mu + \frac{\mu_{\mathrm{t}}}{\sigma_{\varepsilon}}\right)\vec{\nabla}k\right] + c_{1\varepsilon}(P_{\mathrm{k}} + G_{\mathrm{b}})\left(\frac{\varepsilon}{k}\right) - \rho_{\mathrm{a}}c_{2\varepsilon}\left(\frac{\varepsilon^2}{k}\right) \tag{10}$$

where P_{k} is the kinetic energy produced due to turbulence, G_{b} – the turbulence generation due to buoyancy effect, and μ_{t} – the turbulent eddy-viscosity coefficient. These parameters can be determined by:

$$P_{\mathrm{k}} = \mu_{\mathrm{t}} S_{ij} S_{ij}, \quad G_{\mathrm{b}} = -\rho_{\mathrm{a}}\vec{g}\beta\frac{\mu_t}{\sigma}\frac{\partial T}{\partial z} \tag{11}$$

$$\mu_{\mathrm{t}} = c_{\mu}\frac{k^2}{\varepsilon} \tag{12}$$

The constants of the turbulence model are: $\sigma_{\mathrm{k}} = 1.0$, $\sigma_{\varepsilon} = 1.3$, $\sigma_{\mathrm{t}} = 1.0$, $c_{1\varepsilon} = 1.44$, $c_{2\varepsilon} = 1.92$, and $c_{\mu} = 0.09$.

The radiator modelling

When ambient temperature is high, the water spray system begins to spray from around the cooling tower between louvers and radiators (see fig. 1). For heat transfer calculation in the Heller-type heat exchanger (radiator), the e-NTU method is applied [18-20]. The details of computing the heat transfer coefficients, fin efficiency and sedimentation resistance are given in [18-20].

Pressure drop in the air side of the radiators depends on: air flow rate, physical properties of air, angle between air velocity the radiators and *etc*. The air pressure drop passing through deltas, ΔP_{rad} and air pressure drop in the louvers, $\Delta P_{\mathrm{louvers}}$, due to friction of air that passes through the cooling tower skin, ΔP_{skin}, are given in eqs. (13) to (15), respectively [19, 20].

$$\Delta P_{\mathrm{louver}} = 0.000423\left(\frac{C_k^{0.5}G_a}{A_{\mathrm{face}}}\right)^2 \tag{13}$$

$$\Delta P_{\mathrm{rad}} = \left[0.0154 + 0.00073\left(\frac{1}{\sin^2\frac{\alpha}{2}} - 1\right)\right]\left(\frac{C_k^{0.5}G_{\mathrm{a}}}{A_{\mathrm{face}}}\right)^{1.76} \tag{14}$$

$$\Delta P_{\mathrm{skin}} = \frac{\rho_{\mathrm{a},m}}{2}\left[\frac{4G_{\mathrm{a}}}{\pi D_e^2\rho_{\mathrm{a},m}}\right]^2, \quad \rho_{\mathrm{a},m} = 0.5(\rho_{\mathrm{a,in}} + \rho_{\mathrm{a,out}}) \tag{15}$$

Numerical simulation

The NDDCT numerical procedure is categorized into two sections: the 1-D heat exchanger simulation and the numerical solving of the 3-D flow inside and around the cooling tower. The numerical modelling of the radiators has many limitations associated with grid resolution; this is due to the small scale of radiators with respect to the scale of cooling tower, selecting a turbulence model and assigning the boundary conditions. Thus, we use the e-NTU method for computation of the heat transfer in the radiators, coupled with the numerical solution of natural convective turbulent flow through the tower. This heat transfer should be added to the energy equation as a source term (q_r in eq. 6). The total pressures drop of the fluid through the cooling tower, including pressure drop in the louvers and radiators (eqs. 13 and 14) are modelled by the means of putting source term in the momentum equation (*i. e.* F_p in eq. 3). Thus, by e-NTU method and total pressure drop, we may get heat transfer coefficient, h, and pressure drop coefficient, K:

$$\Delta P_{\text{louver}} + \Delta P_{\text{rad}} = K\rho \frac{V_a^2}{2} \tag{16}$$

$$q_{\text{rad}} = hA_{\text{face}}(T_a - T_{\text{rad}}) \tag{17}$$

where V_a is the normal component of air velocity through the radiator face, T_{air} – the air temperature before entering the radiator, and T_{rad} – the temperature of radiator that is equal to the average of the outlet and inlet water flow temperatures. The pressure drop and the heat transfer coefficients may be well correlated with the air velocity based on the given cooling tower type, obtained from eqs. (16) and (17). The heat transfer and pressure drop coefficients for selected radiator are shown in fig. 2.

The conservation equations of momentum, energy and species equations and the phase of water flow droplet are solved by applying the commercial FLUENT software, and by applying a simple computer program for determining the heat transfer and pressure drop in the radiators.

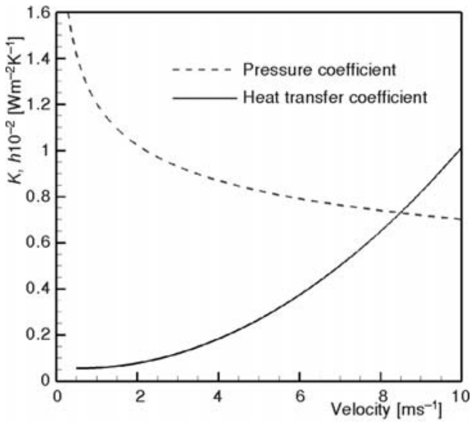

Figure 2. The heat transfer and the pressure drop coefficients as a function of velocity

Analytical solution without crosswind

In order to validate the numerical simulation in NDDCT, an analytical scheme for tower under no-crosswind conditions is developed with water spray effect. The flow in the tower should be assumed to be 1-D. The water spray is assumed to be completely evaporated by an increase in the humidity of the air before entering the cooling tower. The air passing through these small droplets is cooled off and then enters radiators that lead to a decrease in outlet water temperature. Based on the given water spray flow rate, the wet and dry bulb temperatures of the inlet air of radiators is computed using thermodynamic relations of air-vapor mixture. Therefore, the air/water flow in the tower is modelled using one phase. Then, the outlet air temperature of the radiator is guessed and the air velocity through the radiator is estimated. The heat transfer, the pressure drop and the outlet air temperature of the radiator are calculated by applying e-NTU method. Then, the air velocity through the radiator is calculated by eqs. (13), (14), and (16). This process is repeated until the converged solution is obtained, *i. e.*, the difference of computed temperatures becomes negligible [20].

Results and discussion

NDDCT of a power plant that is located in a dry and hot region is simulated numerically (see fig. 1). Heller-type heat exchanger (radiator) of this cooling tower has 119 deltas with

238 radiator columns and 440 tubes with two passes in six rows. The heat is released at the water-side and absorbed at the air side of the heat exchangers. The water temperature at the radiator entry, $T_{\mathrm{w,in}}$ is given, therefore the water temperature at the radiator exit, $T_{\mathrm{w,out}}$, can be calculated by the following equation:

$$q_{\mathrm{rad}} = \dot{m}_{\mathrm{a}} C_{P\mathrm{a}} (T_{\mathrm{a,out}} - T_{\mathrm{a,in}}) = \dot{m}_{\mathrm{w}} C_{P\mathrm{w}} (T_{\mathrm{w,in}} - T_{\mathrm{w,out}}) \tag{18}$$

Here the effect of the sprayed water evaporation rate, outlet water temperature on water spray rate, droplets diameter, spray configuration, ambient temperature, wind velocity, and the distance between the sprayers and the radiators are considered.

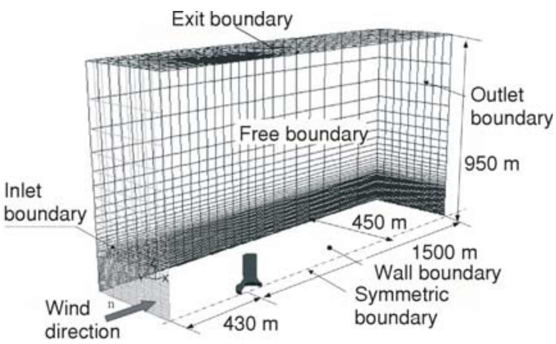

Figure 3. The computational domain and boundary conditions under crosswind

The computational domain, the boundary conditions and the grid system are illustrated in fig. 3. Only half of the flow field was simulated because of the symmetry in geometry, flow, and thermal conditions. Two blocks of grids in the interior and exterior of the tower are adopted in the computation.

The crosswind velocity magnitude, V_{wind}, is obtained according to eq. (19) where the reference elevation, Z_{ref} is 10 m above ground level:

$$V_{\mathrm{wind}} = V_{\mathrm{ref}} \left(\frac{Z}{Z_{\mathrm{ref}}} \right)^{0.16} \tag{19}$$

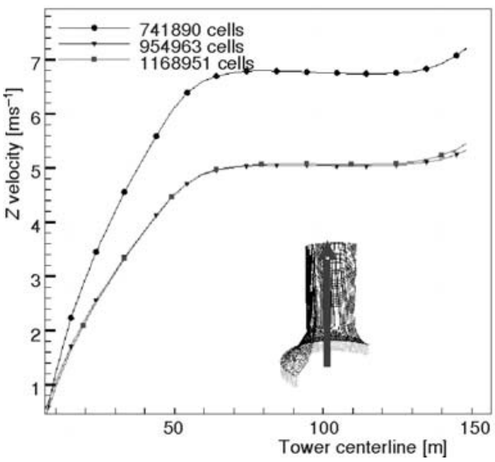

Figure 4. Effect of grid resolution on the vertical velocity in the centerline of the tower

To obtain a grid-independence solution, grid studies are conducted and three different grid resolutions are used, which enables grid studies to be performed and compared. The first case has the coarsest resolution, the second case has a medium resolution and the last one has the finest grid. As an acceptance criterion, wind speed on the vertical velocity in the centerline of the tower was chosen for the above-mentioned different cases (see fig. 4). Here, no deviation is observed in two last ones that gave grid-independent solutions.

Knowing the droplets diameter is important. Droplet diameters depend on water flow rate, water temperature, the nozzle diameter and water pressure. If water droplets hit the radiator, they may deposit on radiator surface. The smaller diameter results in higher evaporation rate, thus, the droplets diameter should be determined in such a way that: (1) the total spray water is evaporated and (2) the water droplets are evaporated before they hit the deltas, so that sedimentation is prevented. The radiators are simulated in 1-D. Therefore, the interaction between radiator walls and water droplets are not modeled here. The difference between the outlet and the inlet water temperatures in the radiator is shown in fig. 5 for different sizes of water droplets and various rates of water spray. Increasing of the water spray rate, lead to an increase in the difference between the inlet and the outlet water temperatures and consequently an increase in the dissipated heat from the radiators. At the water spray rate of 84 kg/s and droplet diameters, d, of 0.1, 1, and 10 μm, the difference between the inlet and the outlet water temperatures of cooling tower is increased approximately 37.2% in comparison with no water spray use condition. However, this ratio was 12.1% for droplets with diameters of 100 μm in the same rate of water spray. Besides, big water droplets hit the radiator and as a result, they may deposit on the surface of the radiator. Since the small droplets experience rapid evaporation, for drops to be prevented to hit on the radiator and to be produced by many commercial sprayers the diameter of 10 μm has been selected for this study. In these conditions, most droplets are evaporated before impinge on the radiators. The radiators are simulated in 1-D. Therefore, the interaction between radiator walls and water droplets are not modeled.

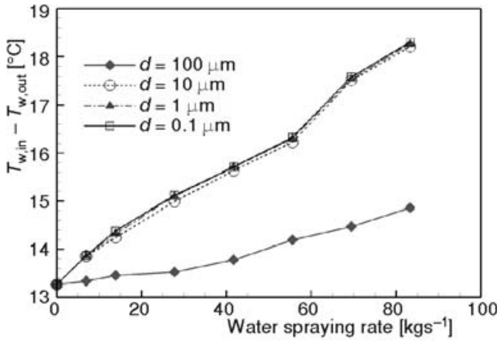

Figure 5. Outlet and inlet water temperature differences for various droplet diameters as a function of water spray flow rate

Comparison of numerical simulation and the analytical scheme

In the analytical scheme, water spray effect is simulated by increasing the air humidity before entering the cooling tower. The air that passes through these small droplets is cooled off and then it enters the radiators causing a reduction in outlet water temperature. With increase of the air relative humidity or water spraying rate, the air temperature is decreased and so does the temperature of the outlet water from the tower.

The difference between the inlet and outlet water temperatures from the radiator that was obtained from analytical and the numerical solutions is shown in fig. 6. Here, the ambient temperature and relative humidity are 37 °C and 20%, respectively. As it can be seen, at low water spray rates, the difference between the analytical and numerical results is greater; this is due to the fact that in the analytical method there is assumed to be a homogeneously water spray system. By increasing the water spray rate, the differences between the analytical and numerical methods coinciding at 100 kg/s water flow rate become zero as shown in fig. 6. Numerical solution of turbulent and two-phase flow in the cooling tower is more time-consuming and difficult to achieve compared to the analytical solution. The results obtained for both cases are very similar with minor differences.

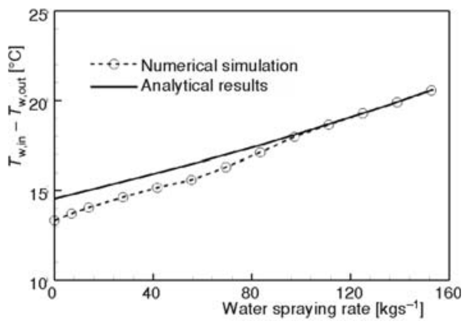

Figure 6. Comparison between the analytical solution and numerical results

Validation of numerical results with no water spray and no crosswind

In order to verify the creditability of numerical results for no water spray and no crosswind, this study compares simulation with the model experiment and the available field

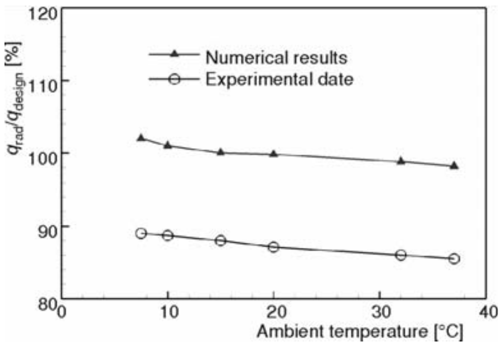

Figure 7. Comparison of computed and experimental heat rejected ratio in the NDDCT [2]

tests [2]. The ratio of predicted heat rejected from the radiators, q_{rad}, to heat rejected in design conditions, q_{design}, is presented in fig. 7, and is defined as:

$$HR = \frac{q_{rad}}{q_{design}} \tag{20}$$

The results show a linear correlation between the ambient temperature and the heat transfer from the heat exchangers with maximum 11% error (see fig. 7). Some discrepancies in the results may be due to applying some simplifications in the modelling of the radiators.

Comparison of the numerical results under crosswind and no water spray conditions

In order to verify the creditability of the numerical simulation for windy and no water spray conditions, this study compares the numerical simulation with the experimental data [2]. The streamlines and velocity vectors on the symmetric plane inside the NDDCT under 15 m/s crosswind velocity are shown in fig. 8. It is clear that there is a "wind-cover" over the tower. The ingoing air flux through the radiator increases in the side facing the wind and decreases in the side surface of the tower; the air discharge at the tower top decreases as well. The crosswind causes the outflow to incline to the downstream. The existence of crosswind causes a reduction in the total heat exchange rate in the windward and leeward of the tower. This is mainly attributed to the airflow around the cooling towers, destroying the radial flow of the surrounding cold air into tower and thus reducing the heat transfer efficiency of the cooling tower. At a relatively low crosswind speed, the air momentum is not too high, and suction effect over the radiators prevents the air separation phenomena inside the tower.

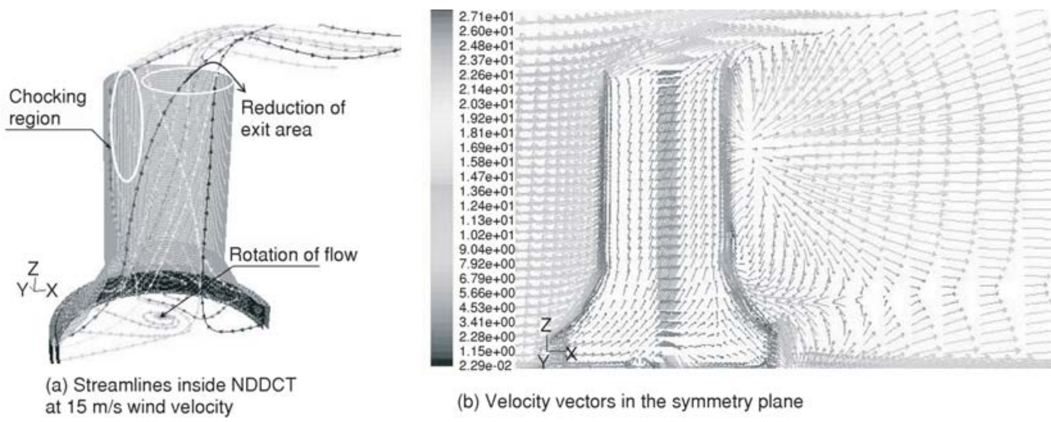

Figure 8. Streamlines and velocity vectors inside the NDDCT under 15 m/s wind velocity

The velocity vectors in the cooling tower base for 15 m/s crosswind velocity are shown in fig. 9. In high wind speeds, a symmetric pair of vortexes may be generated behind the tower due to considerable difference between flow conditions in front and the back of the cooling tower. As illustrated in fig. 9, the outer flow of the tower seems to be like a flow around a circular cylinder. On the side of the tower and outside the radiator, the air tangential velocity is low, so that the flux of air entering into the tower through the radiator is reduced greatly and the air and water temperatures in this part of the radiators are increased. As a result, warm air flows from inside of the tower to the outside and the overall performance of the tower decreases accordingly. Referring to fig. 9, three different zones are detectable near the heat exchangers which are under different crosswind conditions: θ = 0°-60° at front heat exchangers; θ = 60°-120° at side heat exchangers; and θ = 120°-180° at back radiators. The effect of crosswind speed on cooling tower heat transfer is given in tab. 1. With an increase in the wind speed, the symmetric airflow around the tower is disturbed while the pressure drop increases accordingly. Although a low speed wind may slightly increase the tower performance, as a rule, increment of the wind speed reduces the tower efficiency. Existence of an optimum wind speed may be explained by looking at the pressure distribution around the tower. At a relatively low speed, the pressure distribution is not disturbed considerably and the crosswind leads to more airflow over the radiators accordingly.

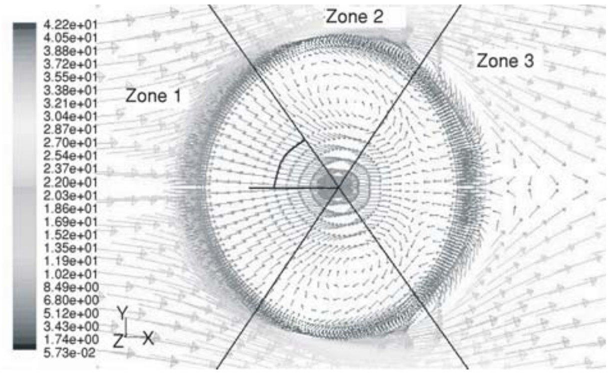

Figure 9. Velocity vectors in the cooling tower base under crosswind velocity of 15 m/s

Table 1. The effect of crosswind speed on the cooling tower heat transfer

Wind velocity [ms^{-1}]	q_{rad} [MW]		
	$\theta_{0°\text{-}60°}$	$\theta_{60°\text{-}120°}$	$\theta_{120°\text{-}180°}$
0	56.6	56.6	56.6
4	58.9	47.6	50.8
10	57.2	22.6	42.7
15	56.9	7.5	30.5

In order to investigate the effect of crosswind on the NDDCT, the cooling tower efficiency is defined as:

$$\text{Efficiency} = \frac{q_{\text{wind}}}{q_{\text{no wind}}} \tag{21}$$

where q_{wind} and $q_{\text{no wind}}$ are both the radiator heat transfer rates under crosswind and no wind, respectively. The numerical results are compared with the experimental data of Du Preez and Kroger [2] in fig. 10. Here, the trend is well predicted by the present numerical modelling and the error in the results is caused by minor difference in the details of the model due to simplifications of model. However, the overall trends are the same, especially the ones regarding the optimum wind velocity, which maximize the cooling tower performance.

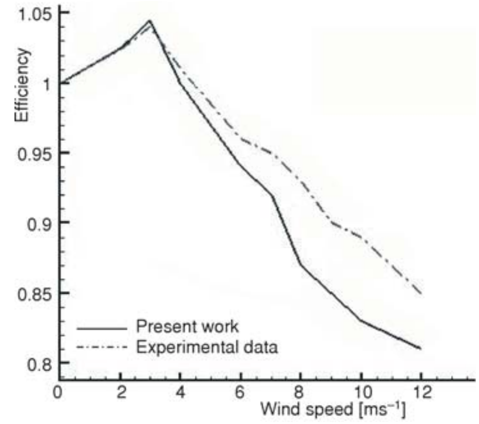

Figure 10. Comparison of the calculated and experimental data of tower efficiency under crosswind speed [2]

Influence of the water spraying on the cooling tower performance

The effect of ambient temperature on the cooling tower efficiency for no crosswind condition is studied in this research when water is sprayed at the cooling tower entrance. The mean evaporation rates of water spray and the outlet and inlet water temperature differences of the cooling tower radiators at both 27 °C and 37 °C of the ambient temperatures are shown in figs. 11 and 12, respectively. The water evaporation rate at both 27 °C and 37 °C ambient temperatures is increased when water is sprayed. Water spray system is more effective at 37 °C ambient temperature. As can be seen in fig. 11, when water-spraying rate is increased, the difference between the evaporation rates of water spraying on the radiator in both 27 °C and 37 °C ambient temperatures is increased. This difference is 23% at 150 kg/s water spray rate. When the ambient temperature is high, the tower performance is decreased. Here, by spraying water on the radiators and decrease the dry bulb temperature of the inlet air that increases the heat transfer rate in the radiator; therefore, the inlet and outlet water temperature difference in the radiator cooling tower is increased (fig. 12).

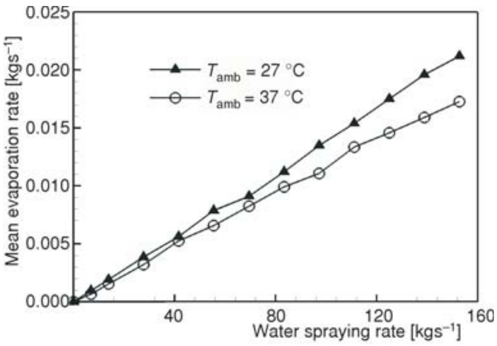

Figure 11. Mean evaporation rate on the radiators as a function of water spray rate

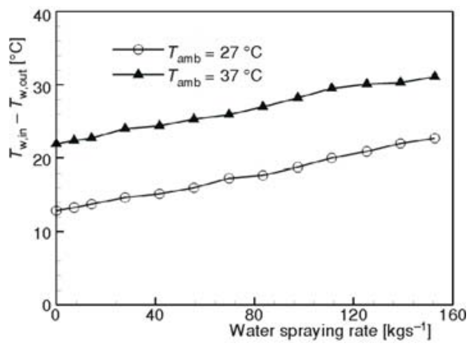

Figure 12. Temperature difference as a function of water spray rate

Simultaneous effects of crosswind and water spray on the cooling tower performance

By investigating the simultaneous crosswind and water spray effect on the NDDCT, the tower performance variation parameter, *TP*, is defined. This is the rejected heat variation from the radiators under the crosswind and water spraying to the no crosswind and no water spraying conditions as:

$$TP = \frac{q_{\text{wind, water spray}} - q_{\text{no wind, no water spray}}}{q_{\text{no wind, no water spray}}} 100 \tag{22}$$

The tower performance variation parameter at various wind velocities for no water spray and water spray flow rates of 25 and 50 kg/s is shown in fig. 13. It is observed that the 3 m/s wind velocity causes a higher efficiency in the cooling system and as was shown, when the wind velocity is lower than 3 m/s, the difference between the inlet and the outlet water temperature from the tower is increased by the wind speed. However, this water temperature decreases when the wind velocity is higher than 3 m/s. For no water spraying and wind velocity of 10 m/s, the heat transfer rate of radiator is 11.5% lower than no wind condition. This value is 7.5% for water spraying rate at 50 kg/s; therefore, water spraying reduces the inefficiency of the crosswind. Here, the portable wind-break walls application is recommended in order to reduce the wind effect when wind velocity exceeds 3 m/s.

It is deduced from fig. 13 that at 10 m/s wind velocity, the cooling tower efficiency is increased by 30% when 50 kg/s water is sprayed on the cooling tower entrance. In this case, the outlet water temperature of the radiators is decreased about 3.5 °C compared to no water spray condition. The tower performance variation parameter at various water-spraying rates is shown in fig. 14 for no wind condition and crosswind velocity of 10 m/s. The difference between these wind velocities is 10.5% and 15% for 0 and 100 kg/s water spraying rates, respectively. Therefore, water spray at the entrance of the NDDCT can increase the performance of the cooling tower in both the no wind and windy conditions.

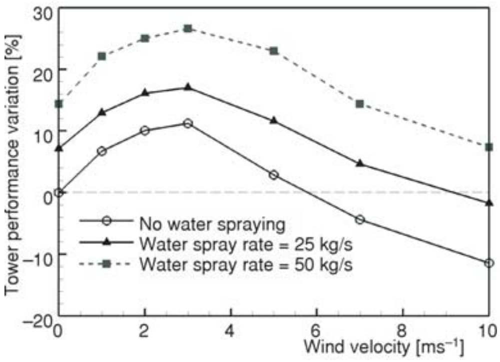

Figure 13. Simultaneous effect of wind velocity and water spraying rate on the NDDCT performance

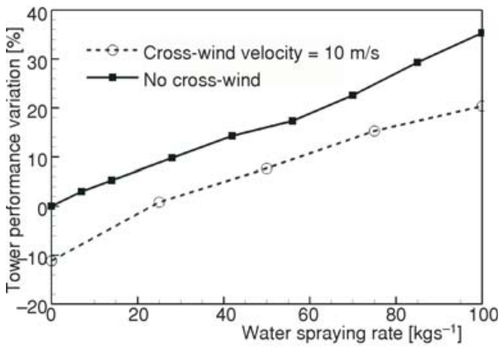

Figure 14. The temperature differences in the radiators as a function of wind velocity

Conclusions

This study investigates the airflow and thermal performance of a NDDCT with and without crosswind. In order to increase the cooling tower efficiency in the hot and dry climate, water spraying at the entrance of the cooling tower is applied. The air that passes through small water drops is cooled and enters the radiators. For windy conditions, simultaneous effect of water spray and cross wind on the performance of NDDCT is studied.

The two-phase flow of the heat and mass transfer inside a NDDCT under crosswind conditions has been simulated here. A comparison has been made between 1-D analytical model and 3-D CFD model for a NDDCT under no wind conditions and when water is sprayed at the cooling entrance. The difference between the predictions of tower cooling range is 8.5% at no water spray condition and it is reduced to zero for high water spray rate. This difference is mostly due to the correlations of the transfer coefficient in the radiators.

Crosswind can significantly reduce the cooling tower efficiency. The numerical simulation of the 3-D fluid flow under crosswind and no water spray is compared with the expected values in the experimental data. The maximum difference between the experimental data and the numerical solution is about 11% in strong wind speed conditions. The results show a significant effect of crosswinds on the NDDCT performance. Under high wind speed conditions, the wind acts as a shield over the tower entrance which leads to reduction of heat transfer through the heat exchangers. The cooling tower efficiency is decreased up to 18% under the influence of crosswind velocity at 12 m/s.

In order to investigate the effect of simultaneous effects of crosswind and water spraying, the variation of heat rejected from the radiators under crosswind and water spraying system on the no crosswind and no water spraying condition are computed. For a given value of water spray rate, at velocities higher than 3 m/s, the crosswind has been found to enhance the thermal performance of the NDDCT, and at velocities lower than 3 m/s, however, crosswinds degrade the NDDCT efficiency. The results show that water spraying reduces the crosswind inefficiency. When wind velocity is increased from zero to 10 m/s, the cooling tower efficiency is decreased about 11.5% and 7.5% for no water spraying and 50 kg/s water spraying rate, respectively.

Acknowledgment

The first author of this article would like to thank from managements of the Shahid Mohammad Montazeri power Station, city of Isfahan, Iran, for providing the cooling tower maps and documents.

Nomenclature

A_{face} – front area of radiators, [m^2]
a_1, a_2, a_3 – consonants of drag coefficient, [–]
C_D – drag coefficient, [–]
C_k – $(=\rho_{\text{amb}}/\rho_{\text{a,m}})$
C_P – specific heat, [Jkg^{-1}K^{-1}]
D_e – diameter, [m]
d_P – diameter of droplets, [mm]
e – effectiveness of a heat exchanger
F_D – volumetric drag force of a particle, [Nm^{-3}]
F_p – force due to pressure drop, [Nm^{-3}]
F_t – volumetric thermophyics force, [Nm^{-3}]
G – mass flow rate, [kgs^{-1}]
G_b – buoyancy turbulence generation, [kgm^{-1}s^{-2}]
g – gravitational acceleration, [ms^{-2}]
h – convective heat transfer coefficient, [Wm^{-2}K^{-1}]
K – pressure loss coefficient in the radiator, [–]
k – turbulent kinetic energy, [m^{2}s^{-2}]
Δm_p – the particle mass change, [kg]
m_p – mass of particle droplet, [kg]
$m_{P,0}$ – initial mass of droplet, [kg]
$\dot{m}_{P,0}$ – mass flow rate of droplets contained in a differential of volume, [kgs^{-1}]
P_k – turbulence kinetic energy production, [kgm^{-1}s^{-2}]
Pr – Prandtl number, [–]
P – pressure, [Nm^{-2}]
q_r – heat source term from the radiators, [Wm^{-3}]
q_{rad} – released heat from the radiators, [W]
q_v – droplets evaporation latent heat, [Wm^{-3}]
r_p – droplet trajectory, [m]
S_m – evaporation source term, [kgm^{3}s^{-1}]
T – temperature, [°C]
t – time, [s]
V – velocity, [ms^{-1}]
V_i – velocity components, [ms^{-1}]
x_i – Cartesian co-ordinates, [m]
Z – elevation from ground level, [m]

Greek symbols

α – delta angel, [–]
β – thermal expansion coefficient, [K^{-1}]
Δ – difference, [–]
ε – turbulent energy dissipation rate, [m^{2}s^{-3}]
μ – viscosity, [kgms^{-1}]
ρ – density, [kgm^{-3}]

Subscripts

a – air
amb – ambient surroundings
eff – effective
in – inlet
m – mean

out	– outlet	ref	– reference
P	– particle (water droplet)	t	– turbulent
rad	– radiator	w	– water

References

[1] du Preez, A. F., Kroger, D. G., Effect of Wind on Performance of a Dry-Cooling Tower, *Heat Recover System and CHP, 13* (1993), 2, pp. 139-146

[2] du Preez, A. F., Kroger, D. G., The Effect of the Heat Exchanger Arrangement and Wind-Break Walls on the Performance of Natural Draft Dry-Cooling Towers Subjected to Crosswinds, *Journal of Wind Engineering and Industrial Aerodynamics, 58* (1995), 3, pp. 293-303

[3] Demuren, O., Rodi, W., Three-Dimensional Numerical Calculations of Flow and Plume Spreading Past Cooling Towers, *Journal of Heat Transfer, 109* (1987), 1, pp. 113-119

[4] Bergstrom, D. J., *et al*., Numerical Study of Wind Flow over a Cooling Tower, *Journal of Wind Engineering and Industrial Aerodynamics, 46-47* (1993), pp. 657-664

[5] Kapas, N., Investigation of Flow Characteristics of Heller-type Cooling Towers with Different Cooling Delta Angels, Periodica Polytechnica ser., *Mechanical Engineering, 47* (2003), 2, pp. 143-150

[6] Kapas, N., Behavior of Natural Draught Cooling Towers in Wind, *Proceedings*, CMFF'03, Budapest, 2003

[7] Al-Waked, R., Behnia, M., The Performance of Natural Draft Dry Cooling Towers under Crosswind: CFD Study, *International Journal of Energy Research, 28* (2004), 2, pp. 147-161

[8] Wei, Q., *et al*., A Study of the Unfavorable Effects of Wind on the Cooling Efficiency of Dry Cooling Towers, *Journal of Wind Engineering and Industrial Aerodynamics, 54-55* (1995), pp. 633-643

[9] Su, M. D., *et al*., Numerical Simulation of Fluid Flow and Thermal Performance of a Dry-Cooling Tower under Cross Wind Condition, *Journal of Wind Engineering and Industrial Aerodynamics, 79* (1999), 3, pp. 289-306

[10] Kaiser, A. S., *et al.*, Numerical Model of Evaporative Cooling Processes in a New Type of Cooling Tower, *International Journal of Heat and Mass Transfer, 48* (2005), 5, pp. 986-999

[11] Javani, M., Ahmadikia, H., Investigation of Natural Draft Dry Cooling Towers Performance under Cross Wind Effect, *Proceedings,* 11th Asian Congress of Fluid Mechanic, Kuala Lumpur, Malaysia, 2006

[12] Zhai, Z., Fu, S., Improving Cooling Efficiency of Dry-Cooling Towers under Crosswind Conditions by using Wind-Break Methods, *Applied Thermal Engineering, 26* (2006), 10, pp. 1008-1017

[13] Mokhtarzadeh-Dehghan, *et al.*, Numerical Study of Single and Two Interacting Turbulent Plumes in Atmospheric Cross Flow, *Atmospheric Environment, 40* (2006), 21, pp. 3909-3923

[14] Lakovic, S. M., *et al*., Impact of the Cold End Operating Condition on Energy Efficiency of the Steam Power Plants, *Thermal Science, 14* (2010), Suppl., pp. S53-S66

[15] Morsi, S. A., Alexander, A. J., An Investigation of Particle Trajectories in Two-Phase Flow Systems, *Journal Fluid Mechanics, 55* (1972), 2, pp. 193-208

[16] Williamson, N. J., Numerical Modelling of Heat and Mass Transfer and Optimization of a Natural Draft Wet Cooling Tower, Ph. D. thesis, University of Sydney, Sydney, Australia, 2008

[17] Williamson, N., *et al*., Comparison of a 2-D Axisymmetric CFD Model of a Natural Draft Wet Cooling Tower and a 1-D Model, *International Journal of Heat and Mass Transfer, 51* (2008), 9-10, pp. 2227-2236

[18] Jaber, H., Webb, R. L., Design of Cooling Towers by the Effectiveness-NTU Method, *Journal of Heat Transfer, 111* (1989), 4, pp. 837-843

[19] ***, Cooling Tower Documents, Isfahan (Shahid Mohammad Montazeri) Thermal Power Plant, 1992

[20] Ahmadikia, H., Iravani, G. A., Numerical Simulation and Analytical Solution of Natural Draft Cooling Tower, *Esteghlal Journal, IUT, 26* (2007), p1, p. 183-195

[21] Hawlader, M. N. A., Liu, B. M., Numerical Study of Thermal-Hydraulic Performance of Evaporative Natural Draft Cooling Towers, *Applied Thermal Engineering, 22* (2002), 1, pp. 41-59

Pape submitted: May 10, 2011
Paper revised: October 10, 2011
Paper accepted: November 12, 2011